Solvation Dynamics at the Interface between Water and Self-assembled Monolayers

John Vieceli and Ilan Benjamin*

Department of Chemistry and Biochemistry, University of California, Santa Cruz, California 95064

Received: October 9, 2002; In Final Form: December 27, 2002

Molecular dynamics computer simulations are used to study the solvation dynamics following an electronic transition in a chromophore adsorbed at the interface between water and chlorine-terminated self-assembled monolayers. By varying the composition of the monolayer and the degree of chlorination, the role of interface polarity and structure on the relaxation time can be elucidated. The relaxation times are found to be faster at smooth interfaces and at interfaces in which the degree of chlorination is larger. Both the water and the self-assembled molecules contribute to the dynamics. However, we find that most of the water contribution to the relaxation is due to water molecules in the first solvent shell while the monolayer contribution is mostly from chlorine-terminated hydrocarbon molecules in the outer solvation shell of the chromophore. The water relaxation is faster than the monolayer relaxation in each system, but it is always slower than that of bulk water. The validity of linear response theory is discussed, and comparisons are made between the relaxation in the systems studied here, simulations of liquid/liquid interfaces, and experimental solvation dynamics data.

I. Introduction

In recent years, advances in nonlinear optical spectroscopies and other surface sensitive techniques[1,2] have enabled us to make much progress in understanding the structure and dynamics of liquid surfaces. However, there are still many open questions concerning the correct microscopic description of the interface, in particular the liquid/liquid and liquid/solid interfaces. One important issue, which we have recently been exploring theoretically, is the relation between the structure of the interface and its ability to solvate and interact with solute molecules which may undergo chemical reactions or simply an electronic transition. Our studies were motivated in part by recent experimental data and, in particular, measurements of static electronic absorption spectra of a chromophore adsorbed at the liquid/liquid[3] and liquid/solid[4] interfaces and measurements of solvation dynamics.[5−9]

Recently, we have been exploring the nature of the interface between water and self-assembled long-chain organic molecules. The interest in these systems is due partially to applications in science and technology.[10,11] For example, one application is in the field of reverse-phase liquid chromatography for the separation of structural isomers.[12] The selectivity of the hydrocarbon phase is dependent on its order, which is measured by the conformation of the hydrocarbon chains (trans versus gauche) and the surface roughness. This type of characterization is directly available from computer simulations of these systems. Besides the intrinsic interest in these systems due to their importance in science and technology, they present an interesting mimic of the interface between water and an organic liquid that is free from the complications due to partial mixing of the two liquids and capillary fluctuations. In addition, they present an environment similar to that of the liquid/solid interface. Another major advantage of these systems is that it is possible to prepare self-assembled monolayers with well characterized molecular structure.[13−15] In particular, one can design the chains with a particular terminal chemical group such as OH, SH, S, Cl, COOH, or NH_2 and thus obtain surfaces with varied structures and physiochemical properties. The interface between these systems and water can be investigated by STM[14] (scanning tunneling microscopy), AFM[14] (atomic force microscopy), neutron reflection,[16] electrochemical techniques, and other thermodynamic and surface characterization methods, such as wetting experiments[17] and nonlinear spectroscopic techniques.[18] In addition, several molecular dynamics studies of water/membrane interfaces and of self-assembled monolayers have been reported,[19−26] but none (other than the previous work from our group[27,28]) have been reported for the spectroscopy of adsorbed and covalently attached chromophores at the interface between them and water. Solvation dynamics in the related systems of an aqueous micellar surface[29−31] and reverse micelles[32,33] have been reported and are compared in section IV to the dynamics at the interface between water and self-assembled monolayers.

In previous publications,[34,27] we have examined the structure and dynamics of the interface between water and self-assembled hydrocarbon chains attached to a silica surface as well as the structure of chemically modified self-assembled hydrocarbon chains in which some or all of the top methyl groups have been substituted with a chlorine atom.[28] Both the structure of the neat interface and the electronic absorption spectra of a chromophore adsorbed at the interface have been calculated and correlated. In the present paper we complete this study by examining the solvation dynamics following a sudden electronic transition in the chromophore. Besides the ability to compare this calculation with recent experimental data, the solvation dynamics enable us to gain further insight into the detailed microscopic interactions at the interface between water and an organic medium with varied structure and polarity.

We consider the interface between water and five different self-assembled hydrocarbon monolayers. The entire terminal methyl group (modeled as united atom) on some or all of the hydrocarbon chains of each monolayer has been substituted by a chlorine atom. The five different systems are designed to have different degrees of roughness by using different length hydrocarbon chains. The partial negative charge on the chlorine atom gives rise to surfaces with different polarity, depending

10.1021/jp0222043 CCC: $25.00
Published on Web 04/23/2003

on the degree of chlorination. As we have demonstrated in an earlier publication,[28] a chromophore adsorbed at these interfaces will be partially solvated by water and the organic phase to a degree that will depend on the roughness of the surface and its polarity. The electronic absorption spectrum of this chromophore shows a signature of all of these interactions. We expect that these will also show up in the dynamic response of the medium to a sudden change in the dipole of the adsorbed chromophore.

We find that the solvation dynamics depend on both the roughness of the surface and its polarity and can be correlated with the shift in the electronic absorption spectra relative to that in bulk water. The dynamics are faster at the smooth surfaces and when the degree of chlorination is larger. By resolving the relaxation into contributions from water and from the organic phase and by looking at these contributions as a function of the distance from the chromophore, we are able to determine that most of the water contribution to the relaxation is due to water molecules in the first solvent shell. The tail of the relaxation is dominated by the slower dynamics of the chain.

The rest of the paper is organized as follows. In section II we discuss the five different interfaces studied and the choice of the potential energy functions. In section III we discuss the methods used to study the solvation dynamics. In section IV we discuss the results of the solvation dynamics calculations and compare them with those of similar interfacial systems and relevant experimental data. Conclusions are presented in section V.

II. System and Potential Energy Functions

The system and potential energy functions have been described previously,[28] and only brief summaries are presented below.

A. Potential Energy Functions. In general, we use pairwise additive intermolecular potentials that are summed over all pairs of sites

$$U(\mathbf{r}) = \sum_{i<j} 4\epsilon_{ij}\left[\left(\frac{\sigma_{ij}}{r_{ij}}\right)^{12} - \left(\frac{\sigma_{ij}}{r_{ij}}\right)^{6}\right] + \frac{q_i q_j}{r_{ij}} \qquad (1)$$

where r_{ij} is the distance between sites i and j, which are in two different molecules, q_i and q_j are the fixed charges on sites i and j, and the Lennard-Jones parameters σ_{ij} and ϵ_{ij} are determined from the parameters of the individual sites according to the usual combination rules for mixtures[35]

$$\sigma_{ij} = \frac{1}{2}(\sigma_i + \sigma_j); \quad \epsilon_{ij} = \sqrt{\epsilon_i \epsilon_j} \qquad (2)$$

In recent years, there have been several papers utilizing many-body polarizable potentials for solvation and charge-transfer studies.[36−38] However, we chose to use nonpolarizable potentials in this work for two reasons: (1) to compare the results with previously published work on solvation dynamics at interfaces that use nonpolarizable potentials;[39,27] (2) to be consistent with the previous work on structure and spectroscopy at the same interfaces.[28] We plan on examining the importance of polarizable potentials in these systems soon.

1. Self-assembled Monolayers. We examine five different chlorine-terminated self-assembled monolayers (SAMs) characterized by different structure and polarity. Each monolayer includes 100 hydrocarbon molecules covalently attached at one end to a Si−O bond of a silica surface. The Si atoms are arranged on a two-dimensional square lattice with a distance of 4.3 Å between neighboring atoms, generating a 43 Å × 43 Å surface. The type and number of each hydrocarbon present on the five different surfaces studied in this work are shown in Table 1. Different surface structures and polarities are generated by varying the ratio of short to long hydrocarbon molecules and the number of chlorine-terminated hydrocarbons present on a surface. Since self-aggregation of hydrocarbon molecules is not observed experimentally,[34] different hydrocarbon types are randomly attached to the silica surface. (Conditions where self-aggregation occurs are possible, but these can be controlled.[40]) The intramolecular and intermolecular potential energy function parameters for the SAMs can be found in our previous publication[28] and references therein.

TABLE 1: Number of Each Hydrocarbon Molecule Used to Construct the Five Self-assembled Monolayers

monolayer	$C_{18}H_{37}$	$C_{17}H_{34}Cl$	$C_{22}H_{45}$	$C_{21}H_{42}Cl$
smooth-all-Cl		100		
smooth-mix-Cl	50	50		
rough-all-Cl		50		50
rough-out-Cl	50			50
rough-in-Cl		50	50	

2. Water and Water−Organic Monolayer Interactions. Each system includes 1000 water molecules on one side of the SAM. The potential energy function for the water is based on the SPC model[41] with the spectroscopic intramolecular potential energy function of Kuchitsu and Morino.[42,28] The potential energy between the water and hydrocarbon molecules is modeled using Lennard-Jones and Coulombic potentials for each pair of atoms. The explicit form of the intramolecular potential energy function and the parameters for the intermolecular potential energy functions have been given elsewhere.[28]

3. Chromophore. The chromophore is a probe of the condensed phase dynamics and is modeled as two atoms held at a fixed distance (using the SHAKE algorithm[43]) of 6 Å, which is a typical charge separation in large dye molecules.[28] Each chromophore atom is assigned a mass of 195 amu, which is a large effective mass corresponding to a large, nearly immobilized chromophore. The charges on the solute atoms, $\pm Q_n$, depend on the electronic state n of the chromophore. The interaction of the chromophore with the water and hydrocarbon atoms is modeled using a sum of Lennard-Jones and Coulombic potentials. The chromophore parameters for the Lennard-Jones potential are taken from a previous publication on methyl-terminated SAMs.[34,27] Since the chromophore is not bound to the monolayer surface, an external window potential is present which restricts the chromophore center of mass to the interface region and prevents diffusion to the bulk water.[28] The use of this potential allows sampling from surface dynamics only, which is consistent with results from experimental surface sensitive detection techniques, such as time-resolved second harmonic generation,[1] and does not interact with the chromophore while it is adsorbed to the monolayer.

B. Boundary Conditions. Periodic boundary conditions are used in the plane parallel to the surface but not in the direction normal to the interface, which creates a water liquid/vapor interface on one end. A reflecting wall is placed in the vapor phase at a distance of approximately 30 Å from the water liquid/vapor interface to prevent the escape of gas phase water molecules and maintain a fixed vapor pressure. All of the intermolecular interactions calculated are smoothly switched to zero using a switching function when the distance between two atoms is between 19.5 and 21.5 Å.[44] Different methodologies for determining the contribution of long-range electrostatic forces have been used recently in studies of water at interfaces, including the two-dimensional and three-dimensional Ewald

summation and the reaction field method. Thermodynamic and transport properties of water at various aqueous interfaces have been calculated using these techniques and were compared with the results using the switching method.[45,46] It was found that convergence of the switching function results to the Ewald method is obtained when the cutoff distance is around 20 Å. In the present work we estimated the contributions to the solute−solvent interaction from distances greater than the cutoff distance to be less than 1% using a uniform reaction field method (with the dielectric constant 82.5, which is that of SPC water[47]). While the contribution to the forces could be somewhat larger, the use of the large cutoff distance in our model suggests that the properties of water have converged. In addition, the solvation dynamics results are expected to be only negligibly affected by the choice of the boundary conditions. Nevertheless, the proper choice of boundary conditions for the study of interfaces is an open issue, especially in systems with large surface charge density. We are currently comparing the switching method employed here with a three-dimensional Ewald summation method for the case of water adjacent to SAMs terminated by carboxylic acid and carboxylate functional groups.

III. Methods

A. Solvation Dynamics. Theoretical studies regarding the dynamic solvent response following a change in the solute electric dipole moment have been performed using continuum electrostatic models, molecular theories, and computer simulations (for recent reviews with an extensive list of references, see refs 48 and 49). In the simulation studies, the solute dipole moment is instantaneously switched from one value to another corresponding to a transition between two electronic states. The solvent molecules respond by reorienting their dipole moments until the equilibrium structure in the final state is reached. The results of the present study correspond to the model chromophore undergoing the $Q = 0.0e \rightarrow Q = 1.0e$ electronic transition, where e is the electron's charge and $+Q$ and $-Q$ are the charges on the two sites of the chromophore. The solvent is equilibrated to the $Q = 0.0e$ state, and the solute charges are switched to the $Q = 1.0e$ state. To quantify the solvent response to this transition, we define the solvent coordinate

$$\Gamma(\mathbf{r}) = \sum_i q_i[(|\mathbf{r}_i - \mathbf{r}_A|)^{-1} - (|\mathbf{r}_i - \mathbf{r}_B|)^{-1}] \qquad (3)$$

where $\mathbf{r}_A$ and $\mathbf{r}_B$ are the positions of the positively and negatively charged solute atoms, respectively, and q_i and $\mathbf{r}_i$ are the atomic charge and position of liquid atom i, respectively. The dynamic solvent coordinate, $\Gamma[\mathbf{r}(t)]$, is used to calculate the nonequilibrium time correlation function of the solvent response following the solute charge transfer, which is given by

$$S(t) = \frac{\overline{\Gamma(t)} - \overline{\Gamma(\infty)}}{\overline{\Gamma(0)} - \overline{\Gamma(\infty)}} \qquad (4)$$

In eq 4, $\overline{\Gamma(t)}$ represents the nonequilibrium ensemble average of $\Gamma[\mathbf{r}(t)]$ at time t. The value of $\overline{\Gamma(0)}$ is equal to the equilibrium average value of the solvent coordinate in the $Q = 0.0e$ state, $\langle\Gamma\rangle_0$, since the solvent is equilibrated to this state initially. The value at $t = \infty$, $\overline{\Gamma(\infty)}$, corresponds to the equilibrium average value of the solvent coordinate in the $Q = 1.0e$ state, $\langle\Gamma\rangle_1$, since the solvent relaxes to this state. The pairwise additive nature of the model potentials allows for contributions from different components of the system to be resolved and is used in the analysis below.

The $S(t)$ calculated from the molecular dynamics simulations may be directly compared with the experimental nonequilibrium time correlation function.

$$\boldsymbol{S}_\omega(t) = \frac{\overline{\omega(t)} - \overline{\omega(\infty)}}{\overline{\omega(0)} - \overline{\omega(\infty)}} \qquad (5)$$

determined from the average time-dependent emission frequency of a photoexcited solute, $\overline{\omega(t)}$. In eq 5, $\overline{\omega(0)}$ and $\overline{\omega(\infty)}$ are the peak frequencies of the static absorption and emission line shapes, respectively.

Once the solvent is equilibrated to the solute in the $Q = 1.0e$ state, the equilibrium fluctuations in $\Gamma(\mathbf{r})$ are used to calculate the equilibrium time correlation function,

$$C(t) = \frac{\langle\{\Gamma[\mathbf{r}(t)] - \langle\Gamma\rangle_1\}\{\Gamma[\mathbf{r}(0)] - \langle\Gamma\rangle_1\}\rangle_1}{\langle\{\Gamma[\mathbf{r}(0)] - \langle\Gamma\rangle_1\}\{\Gamma[\mathbf{r}(0)] - \langle\Gamma\rangle_1\}\rangle_1} \qquad (6)$$

If linear response is assumed, the nonequilibrium solvent response is equal to the equilibrium fluctuations of the solvent in the initial and final solute electronic states,[50−52]

$$S(t) = C(t) \qquad (7)$$

This assumption is valid if the dynamics responsible for the nonequilibrium relaxation are also present in the equilibrium system. The validity of this assumption in these systems is tested below.

B. Simulation Details. Nonequilibrium solvation dynamics following the $Q = 0.0e \rightarrow Q = 1.0e$ electronic transition are studied using fifty trajectories (for each of the five systems), generated from 10 independent initial conditions and run for 5 ps each. Equilibrium solvent fluctuations are determined from a 100 ps simulation. The temperature is 300 K, and all of the simulations are performed using the velocity version of the Verlet algorithm with an integration time step of 0.5 fs.

IV. Solvation Dynamics Results

The normalized nonequilibrium solvent response, $S(t)$, following the chromophore electronic transition $Q = 0.0e \rightarrow Q = 1.0e$ and the normalized equilibrium time correlation function, $C(t)$, in the $Q = 1.0e$ state at the interface with rough (panels A−C) and smooth (panels D and E) monolayers are shown in Figure 1. Since the differences between the systems are evident early in the relaxation, the inset shows the first 0.5 ps of the solvent response. $S(t)$ for each interface is well described by a biexponential decay of the form

$$S(t) = A\exp(-t/\tau_1) + B\exp(-t/\tau_2) \qquad (8)$$

and the same is true for $C(t)$. The parameters from these fits are used to determine the total relaxation times ($\tau_{relax} = A\tau_1 + B\tau_2$) given in Tables 2 and 3 for $S(t)$ and $C(t)$, respectively. For comparison with the interface between water and chlorine-terminated monolayers, Table 2 also shows the relaxation times for the same electronic transition with the same solute in bulk water,[39] at the water/1,2-dichloroethane (DCE) interface (for the normal interface and artificially smooth interface which removes capillary fluctuations)[39] and at the interface between water and methyl-terminated SAMs (smooth-CH_3 and rough-CH_3).[53] After discussing the nonequilibrium results, the equi-

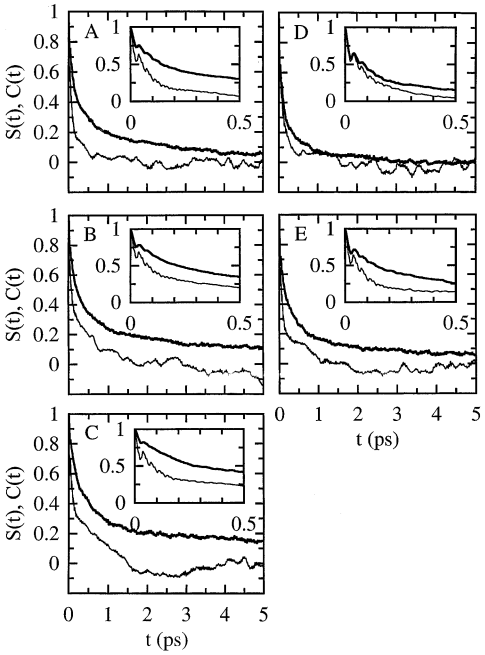

Figure 1. Normalized nonequilibrium ($S(t)$, thick lines) and equilibrium ($C(t)$, thin lines) time correlation functions at the interface between water and (A) rough-all-Cl, (B) rough-out-Cl, (C) rough-in-Cl, (D) smooth-all-Cl, and (E) smooth-mix-Cl. $S(t)$ corresponds to the solvent response following the $Q = 0.0e \rightarrow Q = 1.0e$ electronic transition, and $C(t)$ corresponds to the equilibrium solvent response in the $Q = 1.0e$ state. The insets show the first 0.5 ps of the functions.

TABLE 2: Nonequilibrium Relaxation Times from Fits to $S(t)$ in Figure 1 Using Eq 8 at the Interface between Water and Chlorine-Terminated Self-assembled Monolayers and Results from Other Systems of Interest (As Described in the Text) Shown for Comparison

system	A	τ_1 (ps)	B	τ_2 (ps)	τ_{relax} (ps)
smooth-all-Cl	0.71	0.066	0.29	0.83	0.29
smooth-mix-Cl	0.75	0.14	0.25	2.8	0.81
rough-all-Cl	0.68	0.12	0.32	2.3	0.82
rough-out-Cl	0.70	0.18	0.30	4.1	1.4
rough-in-Cl	0.71	0.26	0.29	6.6	2.1
bulk water	0.49	0.011	0.51	0.27	0.14
water/DCE (normal)	0.59	0.20	0.41	4.5	2.0
water/DCE (smooth)	0.80	0.16	0.20	4.0	0.93
smooth-CH_3	0.63	0.17	0.37	1.4	0.63
rough-CH_3	0.63	0.20	0.37	1.3	0.61

TABLE 3: Equilibrium Relaxation Times from Fits to $C(t)$ in Figure 1 Using Eq 8 at the Interface between Water and Chlorine-Terminated Self-assembled Monolayers

system	A	τ_1 (ps)	B	τ_2 (ps)	τ_{relax} (ps)
smooth-all-Cl	0.78	0.061	0.22	0.53	0.16
smooth-mix-Cl	0.64	0.036	0.36	0.44	0.18
rough-all-Cl	0.73	0.047	0.27	0.41	0.15
rough-out-Cl	0.45	0.024	0.55	0.51	0.29
rough-in-Cl	0.53	0.037	0.47	0.58	0.29

librium correlation functions are used to test the linear response assumption in these systems.

A. Nonequilibrium. Several observations are clear from the nonequilibrium data in Figure 1 and Table 2:

(1) The following trend is observed for τ_{relax} from Table 2 at the five interfaces studied here and several other systems of interest (as described above): bulk water < smooth-all-Cl < smooth-CH_3 ≈ rough-CH_3 < smooth-mix-Cl ≈ water/DCE (smooth) ≈ rough-all-Cl < rough-out-Cl < rough-in-Cl ≈ water/DCE (normal).

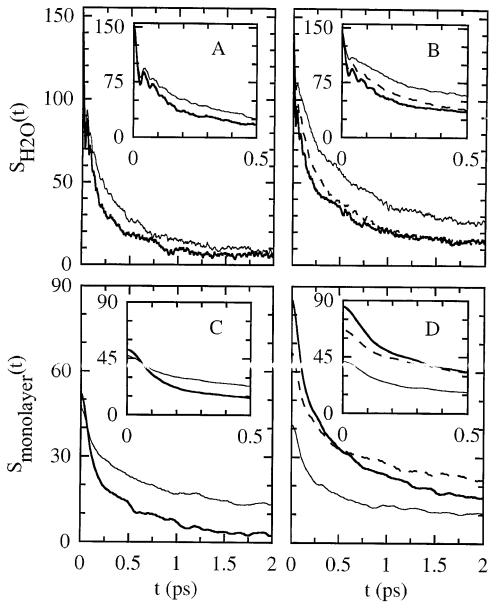

Figure 2. Nonequilibrium time correlation functions resolved into contributions from the water, $S_{H_2O}(t)$, and the monolayer, $S_{SAM}(t)$, following the $Q = 0.0e \rightarrow Q = 1.0e$ electronic transition. Panels A and C correspond to interfaces with smooth monolayers: smooth-all-Cl (thick line) and smooth-mix-Cl (thin line). Panels C and D correspond to the interfaces with rough monolayers: rough-all-Cl (thick line), rough-out-Cl (dashed line), and rough-in-Cl (thin line). The insets show the first 0.5 ps of the functions.

(2) The short time component of τ_{relax} from Table 2 accounts for about 70% of the relaxation at the five interfaces with chlorine-terminated monolayers; however, more significant differences between the systems are evident in the magnitude of τ_2.

(3) At the interface between water and chlorine-terminated SAMs, smooth surfaces relax faster than rough surfaces. The solvation dynamics at the interface between water and methyl-terminated SAMs differ in that smooth-CH_3 and rough-CH_3 relax at almost identical rates.[27]

(4) In the case of both smooth and rough chlorine-terminated surfaces, the relaxation is slower at interfaces where the monolayer is 50% chlorinated than at interfaces with 100% chlorinated monolayers (compare smooth-all-Cl to smooth-mix-Cl and compare rough-all-Cl to the other two rough surfaces).

(5) Differences between the solvent responses are evident as early as 50 fs, indicating the importance of the response from the first solvent shell.

To better understand the observations enumerated above, there are several ways in which the nonequilibrium correlation function can be broken into contributions from different parts of the system. One way utilizes the pairwise additive nature of the model to look at the contributions to $S(t)$ from water, $S_{H_2O}(t)$, and the monolayer, $S_{SAM}(t)$. The data in Figure 2 show the first 2 ps of $S_{H_2O}(t)$ and $S_{SAM}(t)$ at the interface between water and chlorine-terminated monolayers. The normalized functions are also fit using eq 8, and the total relaxation times are shown in Table 4. The relaxation times in Table 4 show that the water response is faster than the monolayer response for all of the systems, but it is always slower than that for bulk water. Differences in the water and monolayer relaxation times between the systems are addressed below, following a characterization of the nonequilibrium time correlation functions.

The functions shown in Figure 2 are not normalized in order to show the contribution of each component to the total relaxation, and thus, they have an initial value corresponding

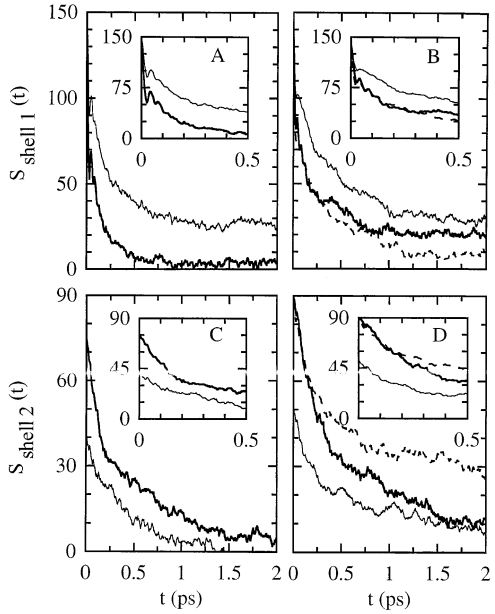

Figure 3. Nonequilibrium time correlation functions resolved into contributions from the first solvent shell, $S_{shell1}(t)$ (as defined in the text), and the outer solvent shells, $S_{shell2}(t)$, following the $Q = 0.0e \rightarrow Q = 1.0e$ electronic transition. The description of the panels and lines is the same as that in Figure 2. The insets show the first 0.5 ps of the functions.

TABLE 4: Nonequilibrium Relaxation Times from Fits to $S_{H2O}(t)$ and $S_{Monolayer}(t)$ in Figure 2 Using Eq 8 at the Interface between Water and Chlorine-terminated Self-assembled Monolayers

system	τ_{relax} (ps) (water)	τ_{relax} (ps) (monolayer)
smooth-all-Cl	0.23	0.44
smooth-mix-Cl	0.40	2.6
rough-all-Cl	0.63	1.1
rough-out-Cl	0.74	3.0
rough-in-Cl	1.9	3.3

to the excess energy in the system from each component (which decays to zero). Since the average electrostatic solvation energy at $t = 0$ is near zero due to the random orientation of the solvent surrounding the chromophore in the $Q = 0.0e$ state, $S(0)$ approximately corresponds to the absolute value of the equilibrium contribution to the solvation energy from each component in the $Q = 1.0e$ state. Consistent with our static adsorption spectra results,[28] the initial values of $S_{H_2O}(t)$ are approximately equal at each interface with a value near 145 kcal/mol. The initial values of $S_{SAM}(t)$ exhibit a range of values, where the most extreme cases are 40 kcal/mol for rough-in-Cl and 85 kcal/mol for rough-all-Cl. In the beginning of the relaxation, water contributes anywhere from 63 to 77% to the total relaxation at these interfaces but the specific partitioning depends on the structure and polarity of the monolayer. The tail of the dynamics in each system is dominated by the monolayer contribution, since it relaxes more slowly than that of the water.

The solvent response can be further characterized by resolving the data into contributions from solvent molecules within the first solvent shell (defined as less than 6 Å), $S_{shell1}(t)$, and those from solvent outside of the first shell (greater than 6 Å but less than 21.5 Å), $S_{shell2}(t)$. Figure 3 shows the data for the first 2 ps of $S_{shell1}(t)$ and $S_{shell2}(t)$. The data are also not normalized in order to show the contribution from each solvent shell to the total relaxation. The first solvent shell contributes anywhere between 56% and 78% to the total relaxation, depending on the monolayer composition. In comparing Figure 3 to Figure 2, a correspondence between the shape of the decay curve for the water response and the first solvent shell response is observed and also between the monolayer response and the outer solvent shell response. From separate equilibrium simulations, the contribution from water to the first solvent shell energy is determined to be greater than 80% in all of the systems while the monolayer contribution to the outer solvent shell energy is 60%−80%. While the water and monolayer responses are not completely accounted for by the first solvent shell and the outer solvent shell, respectively, it is reasonable to conclude from this observation that water molecules in the first solvent shell are dominating the early time dynamics while the monolayer is in the outer solvation shell dominating the long time dynamics.

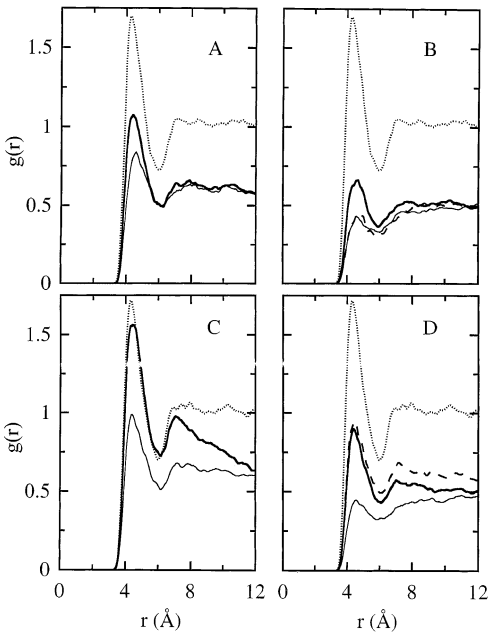

Figure 4. Radial distribution functions between the solute atoms in the $Q = 0.0e$ state and the oxygen from water at the interface with smooth monolayers (panels A and C) and rough monolayers (panels B and D): (A) Smooth-all-Cl (thick line); smooth-mix-Cl (thin line). (B) Rough-all-Cl (thick line); rough-out-Cl (dashed line); rough-in-Cl (thin line). (C) Same as in part A for the other solute atom. (D) Same as in part B for the other solute atom. The dotted line in each panel is for the corresponding data in bulk water.

With the different contributions to the systems characterized, we now focus on the effect of the monolayer roughness and polarity on the nonequilibrium relaxation dynamics of the adjacent water. It is shown above that the water makes a larger contribution to the relaxation than the monolayer in each system. Thus, it is important to understand the relationship between the detailed structure of the interface and the water dynamics. The water relaxation is faster at smooth surfaces than at rough surfaces (with the same percent chlorination) and at 100% chlorinated monolayers relative to 50% chlorinated monolayers (with the same roughness). There are numerous differences between the water structure in each system due to the monolayer structure and polarity (such as surface wetting, density, dipole orientation) that may affect the nonequilibrium dynamics; however, some insight into both of these trends is gained by examining the radial distribution functions (rdfs) of the solute atoms with the oxygen from water when the solute is in the $Q = 0.0e$ state ($t = 0$) and the $Q = 1.0e$ state ($t = \infty$), which are shown in Figures 4 and 5, respectively. The rdfs for the solute in bulk water are also shown for reference. When the solute is in the $Q = 0.0e$ state, the rdfs are different between the systems while the rdfs are nearly identical between the systems when

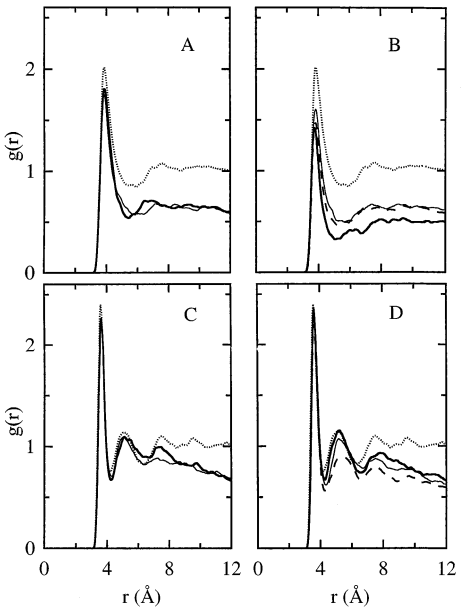

Figure 5. Radial distribution functions between the positively charged solute atom in the $Q = 1.0e$ state and the oxygen from water at the interface with smooth monolayers (panel A) and rough monolayers (panel B). The lines are the same as those in Figure 4. Radial distribution functions for the negatively charged solute atom with the oxygen from water at the interface with smooth monolayers (panel C) and rough monolayers (panel D). The lines are the same as those in Figure 4. The dotted line in each panel is for the corresponding data in bulk water.

TABLE 5: Average First Solvent Shell Peak Height from $g(r)$ for the Solute Atoms in the $Q = 0.0e$ State (Figure 4) and the $Q = 1.0e$ State (Figure 5) with the Oxygen from Water at the Interface between Water and Chlorine-Terminated Self-assembled Monolayers

system	$g(r)_{peak}$ ($Q = 0.0e$)	$g(r)_{peak}$ ($Q = 1.0e$)	ratio
smooth-all-Cl	1.3	2.0	0.65
smooth-mix-Cl	0.91	2.0	0.45
rough-all-Cl	0.78	1.9	0.41
rough-out-Cl	0.70	1.8	0.38
rough-in-Cl	0.44	2.0	0.22
bulk water	1.7	2.2	0.77

the solute is in the $Q = 1.0e$ state. We find that greater similarity between the rdf at $t = 0$ and the rdf at $t = \infty$ results in faster nonequilibrium water relaxation. To quantify the previous statement, the magnitude of the first solvent shell peak (averaged over both solute atoms) from each system is reported in Table 5 for the solute in the $Q = 0.0e$ state and the $Q = 1.0e$ state. The ratio of these two values is also shown. The peak height of the first solvent shell is selected, since water molecules in the first solvent shell make a larger contribution to the nonequilibrium dynamics than those in the outer solvent shells. The data show that an increase in the ratio of the rdf peak height between the initial and final electronic states correlates with faster water relaxation (Table 4). This finding illustrates that the rate of nonequilibrium water relaxation is related to the buildup of the equilibrium solvation structure in the final state. It is shown below that this result is an important factor in the degree of deviation from the linear response assumption in these systems.

Comparison of the nonequilibrium water response from the systems studied here to the results at the interface between water and methyl-terminated monolayers is useful in understanding the effect of an adjacent polar medium on the water relaxation. Table 2 shows that the rate of nonequilibrium solvation

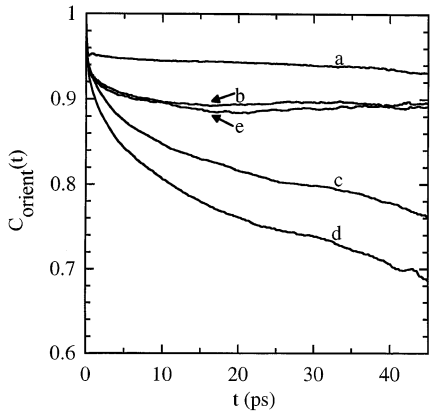

Figure 6. Chlorine-terminated hydrocarbon molecular orientation time correlation functions, $C_{orient}(t)$, defined using the hydrocarbon electric dipole moment from the (a) smooth-all-Cl, (b) smooth-mix-Cl, (c) rough-all-Cl, (d) rough-out-Cl, and (e) rough-in-Cl monolayers.

dynamics at the interface between water and methyl-terminated monolayers, where the only contribution to the dynamics is from the water, is *independent* of the surface roughness.[27] In contrast, increasing the polarity of the media adjacent to water results in a distinction between the water dynamics at smooth and rough interfaces. It has been previously shown that rough surfaces are wetter than smooth surfaces.[34] As the water molecule dipoles that are adjacent to the monolayer on a rough surface reorient following the charge transfer, their response is slowed by the increased interaction with the monolayer dipoles relative to a smooth surface, which exhibits less surface wetting. Since there are no water−surface dipole interactions at the interface with methyl-terminated SAMs, the water response at smooth and rough surfaces is identical. The faster response at smooth chlorine-terminated SAMs relative to rough ones (with the same chlorination) is similar to the result observed at the water/DCE liquid/liquid interface,[54,39] which the chlorine-terminated SAMs attempt to mimic. There it was found that the suppression of capillary fluctuations, which creates a smooth interface, results in faster nonequilibrium relaxation.[39]

The final point to address regarding the nonequilibrium solvation dynamics is the effect of the monolayer roughness and polarity on the monolayer relaxation times. The trend in monolayer relaxation times (Table 4) shows that the relaxation is faster at smooth surfaces relative to rough surfaces (with the same degree of chlorination) and for monolayers with a larger percent chlorination (with the same surface roughness). To better understand the trend among the nonequilibrium monolayer relaxation times and the contribution of the organic monolayer to the solvation dynamics, we examine the reorientation dynamics of the monolayer dipoles. Each chlorinated hydrocarbon molecule contributes a dipole of magnitude 1.9 D (the methyl-terminated hydrocarbons do not contribute to the nonequilibrium relaxation). On a highly ordered monolayer (small number of degrees of freedom), the chlorinated hydrocarbons are expected to exhibit little reorientation in response to a change in the chromophore dipole and, thus, a faster relaxation than that of a more disordered monolayer (higher number of degrees of freedom). If $\hat{\mathbf{r}}$ is a unit vector in the direction of the C−Cl bond on a single chlorine-terminated hydrocarbon molecule, a measure of the molecular orientation dynamics is given by

$$C_{orient}(t) = \langle \hat{\mathbf{r}}(t + \tau) \cdot \hat{\mathbf{r}}(\tau) \rangle \qquad (9)$$

where $\langle\ \rangle$ denotes an average over the chlorine-terminated hydrocarbon molecules and over all time origins, τ. Figure 6

shows $C_{orient}(t)$ for the five monolayers. For monolayers that do not have long chlorine-terminated hydrocarbons (lines a, b, and e), $C_{orient}(t)$ decays to a constant value ($C_{orient}(\infty) > 0$) that is indicative of the range of orientations sampled by the chlorine-terminated hydrocarbon molecules. A $C_{orient}(\infty)$ value closer to 1.0 is associated with a smaller range of orientations. For monolayers with long chlorine-terminated hydrocarbons (lines c and d), the function has not reached an asymptotic value within 45 ps as the system samples a larger range of orientations on a time scale of tens of picoseconds. This interpretation of $C_{orient}(t)$ and the resulting trend are consistent with the trend in nonequilibrium monolayer relaxation times discussed above (with the exception of rough-in-Cl, which is discussed below). The smooth surfaces (lines a and b) exhibit less freedom in the hydrocarbon dipole orientation than rough-all-Cl (line c) and rough-out-Cl (line d) and a faster nonequilibrium relaxation. The increased disorder at these rough surfaces has been characterized previously by broad tilt angle distributions and the presence of gauche defects due to the presence of the long chlorine-terminated hydrocarbons.[28] The data in Figure 6 also show that a larger percent chlorination results in a monolayer with less orientational freedom. The increased charge density on a 100% chlorinated surface restricts the possible hydrocarbon orientations more than those on a 50% chlorinated surface. The result of $C_{orient}(t)$ at the rough-in-Cl (line e) interface is similar to that for smooth-mix-Cl, since the hydrocarbon dipole moment orientation is not affected by adjacent methyl-terminated hydrocarbons that are longer than the chlorine-terminated hydrocarbons. However, the nonequilibrium monolayer response at the rough-in-Cl interface is the slowest of those of the chlorine-terminated monolayers. The additional structural feature of placing the hydrocarbon dipole moments almost 5 Å below those of the long methyl-terminated hydrocarbons at this interface results in nonequilibrium dynamics that do not correlate with the hydrocarbon dipole moment orientation correlation function.

To complete the discussion of solvent molecules' orientation dynamics, eq 9 is used to calculate the equilibrium orientational time correlation function of the single water molecule electric dipole moment in each system as a function of the distance from the monolayer. To do this, the simulation box is divided into several 5 Å regions in the direction perpendicular to the interface. For the smooth surfaces, a "bulk" region and a "surface" region are defined. In addition to these two regions, the "pocket" region is also defined for the rough surfaces, which corresponds to water molecules located between the terminal groups of the short and long hydrocarbon chains. In applying eq 9 to the water molecules, $\hat{\mathbf{r}}$ is the unit vector along the electric dipole moment of a single water molecule and $\langle\ \rangle$ denotes an average over water molecules that were present in the region at the initial time of the trajectory and 5 ps later. The results of these calculations (data not shown) are that, in each of the five systems, the water dipole reorientation in the surface region is slower than that in the bulk region, and the water reorientation in the "pocket" region of the three rough systems is even slower. This is in agreement with previous calculations on water dynamics at surfaces.[32,55] However, an interesting result is that the water dynamics do not depend on the nature of the surface: The reorientation correlation time for the water dipole in the surface region of each of the five systems is around 9 ps. Similarly, the reorientation correlation time for the water dipole in the "pocket" region of each of the three rough systems is around 12 ps (compared with 7 ps in bulk water). These results are in contrast to the water response in the nonequilibrium solvation dynamics, which differs among the five interfacial systems (Table 4). Thus, the collective response of the water molecules to the changing charges is affected by the details of the interfacial system (roughness and polarity) while the single water molecule behavior is not sensitive to these factors in the systems considered here.

B. Testing the Linear Response Assumption. In general, theories of solvation dynamics in bulk liquids used to analyze experimental results are based on the linear response assumption. The assumption is that the nonequilibrium solvent response is equal to the equilibrium solvent fluctuations in the initial or final electronic states of the solute.[50] Using molecular dynamics computer simulations, this assumption has been tested by comparing the nonequilibrium solvent response to the equilibrium solvent fluctuations.[51,52,56−58] Bulk water has been shown to give reasonable agreement with the linear response assumption for a variety of solutes, including monatomic ions[59,60] and polyatomic molecules.[61] Testing of this assumption has also been extended to water/liquid interfaces[39] and the interface between water and methyl-terminated SAMs.[27] The same approach is used here to provide information about the linear response assumption at the interface between water and chlorine-terminated SAMs using the simulation data. Figure 1 shows a comparison of $S(t)$ and $C(t)$ in the systems studied here, with the corresponding relaxation times given in Tables 2 and 3, respectively. The relaxation times obtained from $C(t)$ are similar for the different interfaces, indicating similar dynamics for small fluctuations from equilibrium. This result is supported by the radial distribution functions shown in Figure 5, which indicate that the water solvation structure is similar between the different systems in this electronic state.

In all cases, the nonequilibrium response is slower than the equilibrium one. $S(t)$ calculated at the interface with smooth-all-Cl (panel D) exhibits the smallest deviation from $C(t)$ relative to the other interfaces while rough-in-Cl (panel C) shows the largest deviation between the two functions. The deviation from the linear response assumption in these systems is correlated with loss of the extremely fast oscillatory decay present in $C(t)$. This extremely fast initial relaxation has been observed previously in solvation dynamics studies with water and is attributed to librational modes of the first solvent shell water molecules.[62]

Can the deviation from linear response at these interfaces be attributed to the water, the monolayer, or both components? To answer this, $C(t)$ is resolved into a sum of contributions from the water, $C_{H_2O}(t)$, the monolayer, $C_{SAM}(t)$, and the cross-correlation of the water and monolayer. The cross-correlation function contribution to $C(t)$ is found to be negligible at each interface and is not presented or included in the discussion. (Major contributions from cross-correlation functions have been observed in systems that contain numerous aqueous ions, such as sodium[33] or cesium[29].) In Figure 7, a comparison of the nonequilibrium solvent response for water, $S_{H_2O}(t)$, to the equilibrium fluctuations in the solvent water molecules, $C_{H_2O}(t)$, at each of the interfaces studied is made. We note again that while the equilibrium water response is similar in all the systems, the nonequilibrium response is slower, with the largest slowing-down effect occurring in the rough systems. The data show that loss of the large inertial decay and the oscillatory decay, which is attributed to the librational mode of water molecules in the first solvent shell, contributes to the deviation from the linear response assumption in these systems. This finding is also supported by the radial distribution function between water and the chromophore in the $Q = 0.0e$ state shown in Figure 4. As the peak height of the first solvent shell decreases

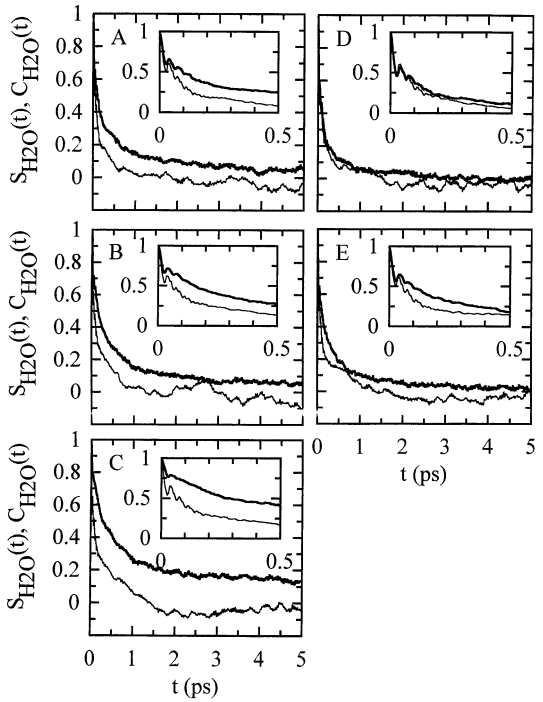

Figure 7. Comparison of the contribution from water to the nonequilibrium ($S_{H_2O}(t)$, thick lines) and equilibrium ($C_{H_2O}(t)$, thin lines) time correlation functions at the interface between water and (A) rough-all-Cl, (B) rough-out-Cl, (C) rough-in-Cl, (D) smooth-all-Cl, and (E) smooth-mix-Cl. $S_{H_2O}(t)$ corresponds to the solvent response following the $Q = 0.0e \rightarrow Q = 1.0e$ electronic transition, and $C_{H_2O}(t)$ corresponds to the equilibrium solvent response in the $Q = 1.0e$ state. The insets show the first 0.5 ps of the functions.

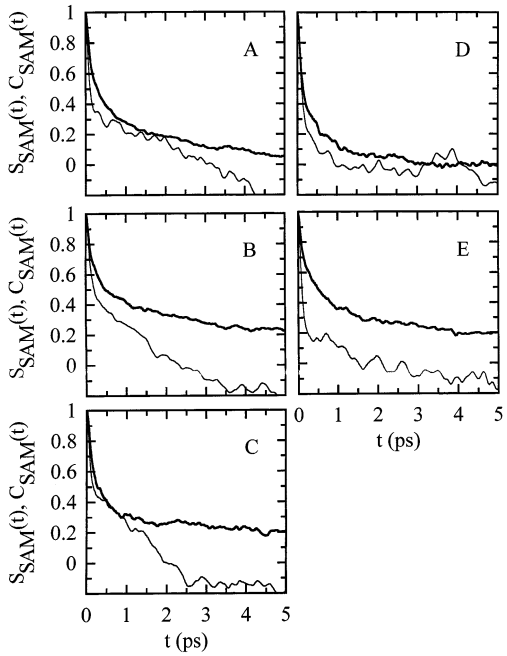

Figure 8. Comparison of the contribution from the chlorine-terminated SAM to the nonequilibrium ($S_{SAM}(t)$, thick lines) and equilibrium ($C_{SAM}(t)$, thin lines) time correlation functions at the interface between water and (A) rough-all-Cl, (B) rough-out-Cl, (C) rough-in-Cl, (D) smooth-all-Cl, and (E) smooth-mix-Cl. $S_{SAM}(t)$ corresponds to the SAM solvent response following the $Q = 0.0e \rightarrow Q = 1.0e$ electronic transition, and $C_{SAM}(t)$ corresponds to the equilibrium SAM solvent response in the $Q = 1.0e$ state.

in the $Q = 0.0e$ state, there is less agreement between $S_{H_2O}(t)$ and $C_{H_2O}(t)$. The initial oscillatory decay present in $C_{H_2O}(t)$ is preserved in $S_{H_2O}(t)$ if the water solvation structure of the initial state in the nonequilibrium process is similar to the structure in the final state.

The corresponding comparison between the nonequilibrium monolayer response and the equilibrium monolayer fluctuations is shown in Figure 8. Relative to the $C_{H_2O}(t)$ shown in Figure 7, $C_{SAM}(t)$ exhibits more statistical noise, since the solute−SAM interaction energy is much smaller than the water−solute interaction energy. The data in Figure 8 show that the SAM also contributes to the deviation from linear response. The deviation begins to show up within several hundreds of femtoseconds but is most prominent in the presence of a longer time component in the nonequilibrium response relative to equilibrium fluctuations. To summarize the data presented in Figures 7 and 8, deviations from the linear response assumption are due to the water in the short time response and the monolayer in the long time response. However, the larger contribution to the interaction energy from the water (in both nonequilibrium and equilibrium) emphasizes the deviation due to the water when comparing $S(t)$ to $C(t)$.

For the same solute undergoing the same electronic transition as in the current study, deviation from linear response in other interfacial systems has been previously observed at liquid/liquid interfaces,[39] and the same relationship between the *C(t)* and the *S(t)* was found at the interface between water and methyl-terminated SAMs,[27] while the results in bulk water show good agreement with linear response.[39] It is interesting to note that solvation dynamics for an ion neutralization reaction ($Cl^- \rightarrow Cl$) at the water liquid/vapor interface[60] show the opposite trend to the one observed here: The nonequilibrium response is the same in the bulk and at the interface and faster than the corresponding equilibrium response, while the equilibrium response is slower at the interface than in the bulk. Even in bulk water $S(t)$ is faster than $C(t)$, as was found by Skaf and Ladanyi,[63] for a dipole flip reaction. On the other hand, a solvation dynamics simulation in aqueous reverse micelles for a solute undergoing a charge shift reaction shows that linear response is valid.[33] Clearly, the nature of the charge-transfer reaction is of crucial importance for determining the validity of linear response and, of course, for the rate of nonequilibrium solvation.[59]

C. Comparison with Relevant Bulk and Interfacial Systems. There are numerous theoretical and experimental studies at interfaces with which this work can be compared, since the structure and spectroscopy indicate that these interfaces are described by features adapted from liquid/liquid and liquid/solid interfaces. Benderskii and Eisenthal have recently used time-resolved second harmonic generation to measure the solvation dynamics of coumarin 314 at a series of water/lipid interfaces. In particular, lipid monolayers of stearic acid,[7] $CH_3(CH_2)_{16}COOH$, stearate,[8] $CH_3(CH_2)_{16}COO^-$, and sodium dodecyl sulfate (SDS),[9] $CH_3(CH_2)_{11}OSO_3^-$, are used. The relaxation times are found to be slower at interfaces with negatively charged lipids relative to the interface with a neutral lipid. The authors correlate the slower response at negatively charged water/lipid interfaces with increased hydrogen bonding and alignment of the interfacial water molecules. These experimental systems include features not present in the simulated systems studied here, such as water−monolayer hydrogen bonding and monolayer net charge, and a direct comparison is reserved for a molecular dynamics simulation of these systems. However, the similar time scales of the solvent response in these experimental systems and the simulated systems studied here indicate that the model used here predicts relaxation times that

are of the correct order of magnitude for this process at this type of interfacial system.

Molecular dynamics simulations of ion solvation dynamics at an aqueous micellar surface have been performed with some similar results to those for the systems studied here.[29,31] Relative to the case of bulk water, the solvation dynamics at a micellar surface are slower by around 2 orders of magnitude. Depending on the SAM composition in our study, a slowing down effect ranging from less than an order of magnitude to around an order of magnitude is observed relative to the case of bulk water (Table 2). The more dramatic slowing down effect at the aqueous micellar surfaces relative to the aqueous interfaces with chlorine-terminated SAMs is likely due to the presence of an ionic probe and ionic headgroups on the surfactant molecules in the micelle studies. Also, the slow component in the solvation dynamics at the micelle surface is due to interactions of the ion with the micellar headgroups and not with the water. A similar finding is observed at the water/SAM interfaces, where the monolayer relaxation times are consistently longer than the water relaxation times in each system (Table 4). Faeder and Ladanyi have simulated the solvation dynamics in aqueous reverse micelles as a function of micellar radius, which also exhibit several similarities to the systems presented in this work.[33] In reverse micelles, the early time dynamics of $S(t)$ ($t < 0.2$ ps) account for about 75% of the decay from the initial value. This large initial decay of $S(t)$ is a characteristic of water solvation dynamics and is also present at the water/SAM interfaces (Figure 2). While the water dynamics are significantly influenced by the micelle radius,[32] the solvation dynamics on a short time scale are nearly independent of the micelle size. The long-time response does, however, depend on the micellar radius. At the water/SAM interfaces, differences in τ_{relax} between the systems are evident in the short time response (Table 2); however, differences in the total relaxation times are primarily due to the contribution from the long time response, since τ_2 is much larger than τ_1. This suggests that the long time response in solvation dynamics at these interfacial environments is more sensitive to the details of the interfacial system than the short time response.

A correspondence has been observed between the solvation dynamics at the water/nonane interface and those at the interface between water and methyl-terminated SAMs, with variations between the two systems attributed to the lack of capillary fluctuations at the water/monolayer interface.[27] The interface with chlorine-terminated monolayers is designed as a mimic of the water/DCE interface, and the correspondence between liquid/liquid and liquid/monolayer interfaces is further tested. Figure 9 shows the solvation dynamics results for the same transition studied here in bulk water and when the solute is located at the Gibbs surface (the plane where the density of each liquid corresponds to approximately 50% of the bulk value) of the water/DCE interface.[39] A comparison of the solvation dynamics at the normal water/DCE interface (line a) and at the interface between water and chlorine-terminated monolayers shows the water/DCE interface results are most similar to those of the interface with rough-in-Cl (line b), although those for the liquid/liquid interface are slightly slower. When the capillary fluctuations are removed to generate a smooth water/DCE interface (line c), the results are similar to the results from the interface between water and the smooth-mix-Cl monolayer (line d). For solvation dynamics, mimics of rough and smooth liquid/liquid interfaces are possible using water/monolayer interfaces with different monolayer chemical composition and structure. Figure 9 also shows the solvation dynamics corresponding to the same transition in bulk water (line e). The slower dynamics at the interfaces studied here relative to bulk water are attributed to both slower water dynamics at the interface and the introduction of the monolayer relaxation, which is slower than the water relaxation in each system.

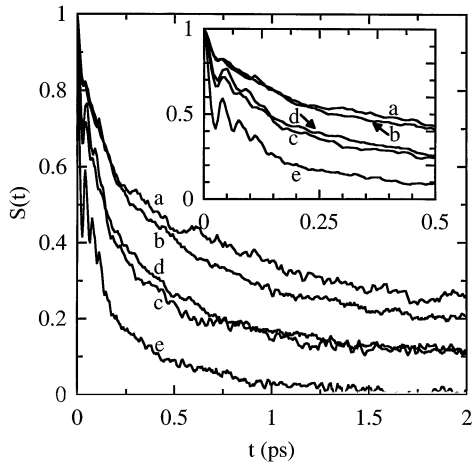

Figure 9. Comparison of the normalized nonequilibrium time correlation functions, $S(t)$, in several different systems following the $Q = 0.0e \rightarrow Q = 1.0e$ electronic transition. The different lines correspond to (a) the normal water/1,2-dichlorethane interface, (b) the water/rough-in-Cl interface, (c) the smooth water/1,2-dichloroethane interface, where capillary fluctuations are removed, (d) the water/smooth-mix-Cl interface, and (e) bulk water. The inset shows the first 0.5 ps of the functions.

V. Conclusions

Solvation dynamics at the interface between water and chlorine-terminated SAMs are studied to understand the role of monolayer polarity and roughness on the relaxation time. The relaxation times are found to be faster at interfaces with smooth monolayers and at interfaces in which the monolayer percent chlorination is larger. The data are resolved into contributions from the water and the monolayer and also into contributions from the different solvent shells. The water relaxation is faster than the monolayer relaxation in each system, but it is always slower than that of bulk water. Most of the water contribution to the relaxation is due to water molecules in the first solvent shell while the monolayer contribution is mostly from chlorine-terminated hydrocarbon molecules in the outer solvent shell. The validity of the linear response assumption in these systems is tested by comparing the nonequilibrium solvent response following an electronic transition to the equilibrium fluctuations in the solvent. Deviation from the linear response assumption is attributed mostly to loss of the initial oscillatory decay, which is present in the equilibrium time correlation function and attributed to librational modes of the first solvent shell water molecules. The systems studied here are also designed as a mimic of the normal and artificially smooth water/DCE interface. A correspondence between the solvation dynamics results is observed between the normal water/DCE interface (with capillary fluctuations) and a rough water/monolayer interface and also between the artificially smooth water/DCE interface (where capillary fluctuations are removed) and a smooth water/monolayer interface.

Acknowledgment. This work has been supported by a grant from the National Science Foundation (CHE-9981847).

References and Notes

(1) Eisenthal, K. B. *Chem. Rev.* **1996**, *96*, 1343.
(2) Richmond, G. L. *Annu. Rev. Phys. Chem.* **2001**, *52*, 357.

(3) Wang, H.; Borguet, E.; Eisenthal, K. B. *J. Phys. Chem.* **1997**, *101*, 713.
(4) Zhang, X.; Walker, R. A. *Langmuir* **2001**, *17*, 4486.
(5) Zimdars, D.; Dadap, J. I.; Eisenthal, K. B.; Heinz, T. F. *Chem. Phys. Lett.* **1999**, *301*, 112.
(6) Zimdars, D.; Eisenthal, K. B. *J. Phys. Chem. A* **1999**, *103*, 10567.
(7) Benderskii, A. V.; Eisenthal, K. B. *J. Phys. Chem. B* **2000**, *104*, 11723.
(8) Benderskii, A. V.; Eisenthal, K. B. *J. Phys, Chem, B* **2001**, *105*, 6698.
(9) Benderskii, A. V.; Eisenthal, K. B. *J. Phys. Chem. A* **2002**, *106*, 7482.
(10) Evans, D.; Wampler, R. *J. Phys. Chem. B* **1999**, *103*, 4666.
(11) Kaschak, D. M.; Mallouk, T. E. *J. Am. Chem. Soc.* **1996**, *118*, 4222.
(12) Pursch, M.; Vanderhart, D. L.; Sander, L. C.; Gu, X.; Nguyen, T.; Wise, S. A.; Gajewski, D. A. *J. Am. Chem. Soc.* **2000**, *122*, 6997.
(13) Whitesides, G. M.; Laibinis, P. E. *Langmuir* **1990**, *6*, 87.
(14) Giancarlo, L. C.; Flynn, G. W. *Annu. Rev. Phys. Chem.* **1998**, *49*, 297.
(15) Brunner, H.; Vallant, T.; Mayer, U.; Hoffmann, H. *Surf. Sci.* **1996**, *368*, 279.
(16) Lu, J. R.; Thomas, R. K. *J. Chem. Soc., Faraday Trans.* **1998**, *94*, 995.
(17) Olbris, D. J.; Ulman, A.; Shnidman, Y. *J. Chem. Phys.* **1995**, *102*, 6865.
(18) Eisert, F.; Dannenberger, O.; Buck, M. *Phys. Rev. B* **1998**, *58*, 10860.
(19) Hautman, J.; Bareman, J. P.; Mar, W.; Klein, M. L. *J. Chem. Soc., Faraday Trans.* **1991**, *87*, 2031.
(20) Stouch, T. R. *Mol. Simul.* **1993**, *10*, 335.
(21) Venable, R. M.; Zhang, Y. H.; Hardy, B. J.; Pastor, R. W. *Science* **1993**, *262*, 223.
(22) Marrink, S. J.; Berkowitz, M.; Berendsen, H. J. C. *Langmuir* **1993**, *9*, 3122.
(23) Mar, W.; Klein, M. L. *Langmuir* **1994**, *10*, 188.
(24) Pohorille, A.; Wilson, M. A. *Origins Life Evol. Biosphere* **1994**, *25*, 21.
(25) Schulten, K.; Zhou, F. *J. Phys. Chem.* **1995**, *99*, 2194.
(26) Tobias, D. J.; Tu, K. C.; Klein, M. L. *Curr. Opin. Colloid Interface Sci.* **1997**, *2*, 15.
(27) Squitieri, E.; Benjamin, I. *J. Phys. Chem. B* **2001**, *105*, 6412.
(28) Vieceli, J.; Benjamin, I. *J. Phys. Chem. B* **2002**, *106*, 7898.
(29) Balasubramanian, S.; Bagchi, B. *J. Phys. Chem. B* **2001**, *105*, 12529.
(30) Balasubramanian, S.; Bagchi, B. *J. Phys. Chem. B* **2002**, *106*, 3668.
(31) Pal, S.; Balasubramanian, S.; Bagchi, B. *J. Chem. Phys.* **2002**, *117*, 2852.
(32) Faeder, J.; Ladanyi, B. M. *J. Phys. Chem. B* **2000**, *104*, 1033.
(33) Faeder, J.; Ladanyi, B. M. *J. Chem. Phys. B* **2001**, *105*, 11148.
(34) Rudich, Y.; Benjamin, I.; Naaman, R.; Thomas, E.; Trakhtenberg, S.; Ussyshkin, R. *J. Phys. Chem. A* **2000**, *104*, 5238.
(35) Hansen, J.-P.; McDonald, I. R. *Theory of Simple Liquids*, 2nd ed.; Academic: London, 1986.
(36) King, G.; Warshel, A. *J. Chem. Phys.* **1990**, *93*, 8682.
(37) Bader, J. S.; Berne, B. J. *J. Chem. Phys.* **1996**, *104*, 1293.
(38) Dang, L. X.; Chang, T. *J. Phys. Chem. B* **2002**, *106*, 235.
(39) Michael, D.; Benjamin, I. *J. Chem. Phys.* **2001**, *114*, 2817.
(40) Lagutchev, A. S.; Song, K. J.; Huang, J. Y.; Yang, P. K.; Chuang, T. J. *Surf. Coat. Technol.* **1997**, *94*−*95*, 383.
(41) Berendsen, H. J. C.; Postma, J. P. M.; Gunsteren, W. F. V.; Hermans, J. In *Intermolecular Forces*; Pullman, B., Ed.; D. Reidel: Dordrecht, 1981; p 331.
(42) Kuchitsu, K.; Morino, Y. *Bull. Chem. Soc. Jpn.* **1965**, *38*, 814.
(43) Ciccotti, G.; Ferrario, M.; Hynes, J. T.; Kapral, R. *Chem. Phys.* **1989**, *129*, 241.
(44) Allen, M. P.; Tildesley, D. J. *Computer Simulation of Liquids*; Clarendon: Oxford, 1987.
(45) Spohr, E. *J. Chem. Phys.* **1997**, *107*, 6342.
(46) Feller, S. E.; Pastor, R. W.; Rojnuckarin, A.; Bogusz, S.; Brooks, B. R. *J. Phys. Chem.* **1996**, *100*, 17011.
(47) Anderson, J.; Ullo, J. J.; Yip, S. *J. Chem. Phys.* **1987**, *87*, 1726.
(48) Stratt, M.; Maroncelli, M. *J. Phys. Chem.* **1996**, *100*, 12981.
(49) Nandi, N.; Bhattacharyya, K.; Bagchi, B. *Chem. Rev.* **2000**, *100*, 2013.
(50) Chandler, D. *Introduction to Modern Statistical Mechanics*; Oxford University Press: Oxford, 1987.
(51) Carter, E. A.; Hynes, J. T. *J. Chem. Phys.* **1991**, *94*, 5961.
(52) Stephens, M. D.; Saven, J. G.; Skinner, J. L. *J. Chem. Phys.* **1997**, *106*, 2129.
(53) Squitieri, E.; Benjamin, I. *J. Phys. Chem. B* **2001**, *105*, 6412. Rough-CH_3 from this publication refers to the case when the solute is covalently attached to the long hydrocarbon molecule. Attachment to the short hydrocarbon molecule is not considered here, since this involves the effect of burying the chromophore in the monolayer, which is not consistent with the solute location at the interfaces with chlorine-terminated monolayers where it is physically adsorbed.
(54) Benjamin, I. *J. Chem. Phys.* **1992**, *97*, 1432.
(55) Benjamin, I. Molecular dynamics simulations in interfacial electrochemistry. In *Modern Aspects of Electrochemistry*; Bockris, J. O. M., Conway, B. E., White, R. E., Eds.; Plenum Press: New York, 1997; Vol. 31, p 115.
(56) Fonseca, T.; Ladanyi, B. M. *J. Phys. Chem.* **1991**, *95*, 2116.
(57) Tran, V.; Schwartz, B. J. *J. Phys. Chem. B* **1999**, *103*, 5570.
(58) Geissler, P. L.; Chandler, D. *J. Chem. Phys.* **2000**, *113*, 9759.
(59) Maroncelli, M.; Fleming, G. R. *J. Chem. Phys.* **1988**, *89*, 5044.
(60) Benjamin, I. *J. Chem. Phys.* **1991**, *95*, 3698.
(61) Ando, K.; Kato, S. *J. Chem. Phys.* **1991**, *95*, 5966.
(62) Maroncelli, M. *J. Mol. Liq.* **1993**, *57*, 1.
(63) Skaf, M. S.; Ladanyi, B. M. *J. Phys. Chem.* **1996**, *100*, 18258.